Eur. Phys. J. D **41**, 563–569 (2007)
DOI: 10.1140/epjd/e2006-00258-0

THE EUROPEAN PHYSICAL JOURNAL D

Enhanced narrow spectral line and double electromagnetically induced two-photon transparency induced by double dark resonances

J.H. Li[a] and X.X. Yang

Department of Physics, Huazhong University of Science and Technology, Wuhan 430074, P.R. China

Received 19 August 2006 / Received in final form 19 October 2006
Published online 8 December 2006 –

Abstract. We theoretically investigate the features of two-photon absorption in a five-level atomic system with interacting dark resonances. It is found that two-photon absorption can be completely suppressed at two different frequencies due to the application of two coherent coupling fields and the atomic system exhibits double electromagnetically induced transparency windows against two-photon absorption. The position and width of the double two-photon transparency windows can be controlled via properly adjusting the frequency detuning and the intensities of the two coupling fields. In addition, one enhanced narrow central line can be observed in the two-photon absorption spectra, which may find applications in high-precision spectroscopy. Form a physical point of view, we explicitly explain these results in terms of quantum interference induced by three different two-photon excitation channels in the dressed-state picture.

PACS. 42.50.Hz Strong-field excitation of optical transitions in quantum systems; multiphoton processes; dynamic Stark shift – 42.50.Gy Effects of atomic coherence on propagation, absorption, and amplification of light; electromagnetically induced transparency and absorption

Effects of atomic coherence and quantum interference are currently becoming an important and intensive tool in resonant nonlinear optical physics. The inhibition of two-photon and multiphoton absorption based on these effects in nonlinear optical regime has potential applications in high-efficiency generation of short-wave length coherent radiation at pump intensities approaching the single-photon level [1–7], trapping and manipulating photon states in atomic ensembles [8], nonlinear spectra at very low light intensity [9–17], ultraslow optical solitons in highly resonant media [18], and pulse-preserving propagation in dissipative media [19,20], and so on. In particular, nonlinear optics assisted by electromagnetically induced transparency (EIT) under few-photon optical field due to extremely large Kerr nonlinearities and refractive-index enhancement without absorption has been already observed [21], and this opens up the possibilities for a new regime of quantum nonlinear optics. For example, Harris et al. proposed the use of EIT to suppress absorption of the short-wavelength light generated in a four-wave mixing (FWM) scheme and showed that the FWM efficiency could be greatly enhanced [1]. Agarwal and Harshawardhan showed that in a four-level Y-type system, two-photon absorption could be selectively suppressed or enhanced [9], and later Gao et al. reported the experimental observation of the electromagnetically induced inhibition of two-photon absorption with atomic sodium vapor as a test medium [10]. In a recent experiment, Yan et al. demonstrated that EIT in a standard Λ-type configuration could be used to suppress both single-photon and two-photon absorptions simultaneously [22,23]. Later on, Wu et al. investigated and discussed a four-wave-mixing (FWM) scheme in a five-level atomic system and hyper-Raman scattering (HRS) in resonant coherent media by the use of EIT, which led to suppressing both two-photon and three-photon absorptions in both FWM and HRS schemes and enabling the four-wave mixing to proceed through real, resonant intermediate states without absorption loss [2]. Quite recently, he and his coworkers again analyzed a lifetime-broadened four-state FWM scheme in the ultraslow propagation regime and put forward a new type of induced transparency resulted from multiphoton destructive interference [24]. In reference [25], Zou et al. investigated two-photon absorption in a three-level ladder atomic system driven by a pair of bichromatic fields of equal frequency differences and demonstrated the reduction of two-absorption absorption.

On the other hand, in recent years a variety of four-level atomic systems driven by three fields have also shown that the probe absorption can be characterized by double-dark resonances [6,26–32]. For the presence of double-dark resonances, there are basically two different kinds of atomic configuration. One kind is Λ-configuration system where the final state has twofold levels, the other kind is a tripod atomic system. The interaction of double-dark states has given rise to some original and significant

[a] e-mail: huajia_li@163.com

effects. For example, Lukin et al. have shown that in a Λ-configuration system where the final state has twofold levels the interaction of double-dark states can result in a splitting of dark states and the appearance of sharp spectral features [26]. Recently, Gong and his coworkers have shown that in the above Λ-configuration four-level system the presence of double-dark states makes it possible to prepare arbitrary coherent superposition states with equal amplitudes but inverse relative phases, even though the condition of multiphoton resonance is not satisfied [28]. More recently, they have also proposed high efficiency four-wave mixing induced by double-dark resonances in a five-level system [6]. Yelin et al. experimentally show and theoretically confirm that double dark resonances lead to the possibility of extremely sharp resonances prevailing even in the presence of considerable Doppler broadening [30]. Alternatively, Goren et al. have studied the sub-Doppler and subnatural narrowing of the absorption line induced by interacting dark resonances in a tripod system [31]. Paspalakis et al. have analyzed coherent propagation and nonlinear generation dynamics in a coherently prepared four-level tripod system [32].

In this paper, we study the two-photon absorption spectra in a five-level atomic system in the presence of double dark resonances. The two-frequency transparency against two-photon absorption occurs in such a system, which expands the frequency range of two-photon transparency and may improve the controllability of two-photon transparency. The position and width of two-frequency transparency windows can be manipulated via appropriately modulating the frequency detuning and the intensities of the two coupling fields. Interestingly enough, one enhanced narrow central line can be observed in the two-photon absorption spectra, which may find applications in high-precision spectroscopy.

Let us consider a five-level atomic system driven by four coherent laser fields, as shown in Figure 1. The atomic levels are labeled as $|0\rangle$, $|1\rangle$, $|2\rangle$, $|3\rangle$, and $|4\rangle$, respectively. A probe laser field E_p (carrier frequency ω_p and Rabi frequency $2\Omega_p$) is applied to the transition $|0\rangle \leftrightarrow |3\rangle$ to serve as the first step of the two-photon excitation of upper atomic state $|4\rangle$. A signal laser field E_s (carrier frequency ω_s and Rabi frequency $2\Omega_s$) is coupled to the transition $|3\rangle \leftrightarrow |4\rangle$ to complete the two-photon excitation of atomic state $|4\rangle$. The transitions $|2\rangle \leftrightarrow |3\rangle$ and $|1\rangle \leftrightarrow |3\rangle$ are respectively driven by two coherent coupling laser fields with Rabi frequencies $2\Omega_c$ and $2\Omega_d$ (amplitudes E_c, E_d and carrier frequencies ω_c, ω_d), which can produce double-dark resonances. In the interaction picture and under the electro-dipole interaction and rotating-wave approximation, with the assumption of $\hbar = 1$, the semiclassical Hamiltonian describing the atom-field interaction for the system under study can be written as

$$\begin{aligned} H_{int} = {} & (\Delta_p - \Delta_d)\,|1\rangle\langle 1| + (\Delta_p - \Delta_c)\,|2\rangle\langle 2| \\ & + \Delta_p|3\rangle\langle 3| + (\Delta_p + \Delta_s)\,|4\rangle\langle 4| \\ & - (\Omega_p|3\rangle\langle 0| + \Omega_s|4\rangle\langle 3| + \Omega_c|3\rangle\langle 2| + \Omega_d|3\rangle\langle 1| + h.c.)\,, \quad (1) \end{aligned}$$

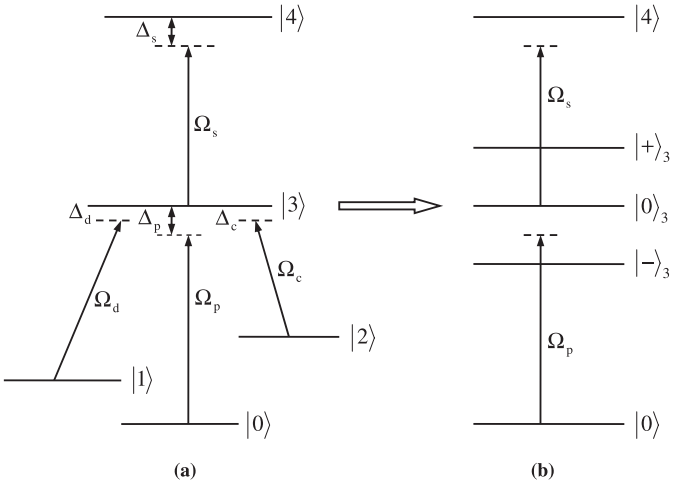

Fig. 1. (a) Schematic diagram of five-level atoms in a resonant coherent medium interacting with a probe laser with Rabi frequency $2\Omega_p$, a signal laser with Rabi frequency $2\Omega_s$, two coupling lasers with Rabi frequencies $2\Omega_c$ and $2\Omega_d$. The atomic levels are labeled as $|0\rangle$, $|1\rangle$, $|2\rangle$, $|3\rangle$, and $|4\rangle$, respectively. The tripod configuration $|0\rangle \rightarrow |3\rangle$, $|1\rangle \rightarrow |3\rangle$, and $|2\rangle \rightarrow |3\rangle$ owns the property of double-dark resonances [31,32]. Δ_p, Δ_s, Δ_c, and Δ_d are the frequency detunings of the corresponding probe, signal, and coupling fields, see text for details. (b) Corresponding dressed-state picture of two coupling fields Ω_c and Ω_d.

where *h.c.* means Hermitian conjugation and for the sake of simplicity we have taken the ground state $|0\rangle$ as the energy origin. The quantities Ω_n $(n = p, s, c, d)$ stand for one-half Rabi frequencies for the respective transitions, i.e., $\Omega_p = d_{30}E_p/(2\hbar)$, $\Omega_s = d_{43}E_s/(2\hbar)$, $\Omega_c = d_{32}E_c/(2\hbar)$, and $\Omega_d = d_{31}E_d/(2\hbar)$, where $d_{ij} = \vec{d}_{ij} \cdot \hat{e}_L$ ($\hat{e}_L$ is the polarization unit vector of the laser field) denotes the dipole moment for the transition between levels $|i\rangle$ and $|j\rangle$. $\Delta_p = \omega_{30} - \omega_p$, $\Delta_s = \omega_{43} - \omega_s$, $\Delta_c = \omega_{32} - \omega_c$ and $\Delta_d = \omega_{31} - \omega_d$, are the frequency detunings of the four coherent fields from the corresponding two-level transitions (see Fig. 1). The decay rates from the states $|4\rangle$ to $|3\rangle$, $|3\rangle$ to $|0\rangle$, $|3\rangle$ to $|1\rangle$, and $|3\rangle$ to $|2\rangle$ are γ_{43}, γ_{30}, γ_{31}, and γ_{32}, respectively. The relaxation rates of coherence between the ground states $|0\rangle$, $|1\rangle$, and $|2\rangle$ are negligible and thus can be safely neglected.

In what follows, using the density-matrix formalism we begin to describe the dynamic response of the resonant coherent medium under study. By the standard approach [33], we can easily obtain the time-dependent density matrix equations of motion as follows:

$$\begin{aligned} \dot{\rho}_{00} &= \gamma_{30}\rho_{33} + i\Omega_p\,(\rho_{30} - \rho_{03})\,, \\ \dot{\rho}_{11} &= \gamma_{31}\rho_{33} + i\Omega_d\,(\rho_{31} - \rho_{13})\,, \\ \dot{\rho}_{22} &= \gamma_{32}\rho_{33} + i\Omega_c\,(\rho_{32} - \rho_{23})\,, \\ \dot{\rho}_{33} &= -\,(\gamma_{30} + \gamma_{31} + \gamma_{32})\,\rho_{33} + \gamma_{43}\rho_{44} + i\Omega_p\,(\rho_{03} - \rho_{30}) \\ &\quad + i\Omega_s\,(\rho_{43} - \rho_{34}) + i\Omega_c\,(\rho_{23} - \rho_{32}) + i\Omega_d\,(\rho_{13} - \rho_{31})\,, \\ \dot{\rho}_{44} &= -\gamma_{43}\rho_{44} + i\Omega_s\,(\rho_{34} - \rho_{43})\,, \\ \dot{\rho}_{01} &= i\,(\Delta_p - \Delta_d)\,\rho_{01} + i\Omega_p\rho_{31} - i\Omega_d\rho_{03}, \end{aligned}$$

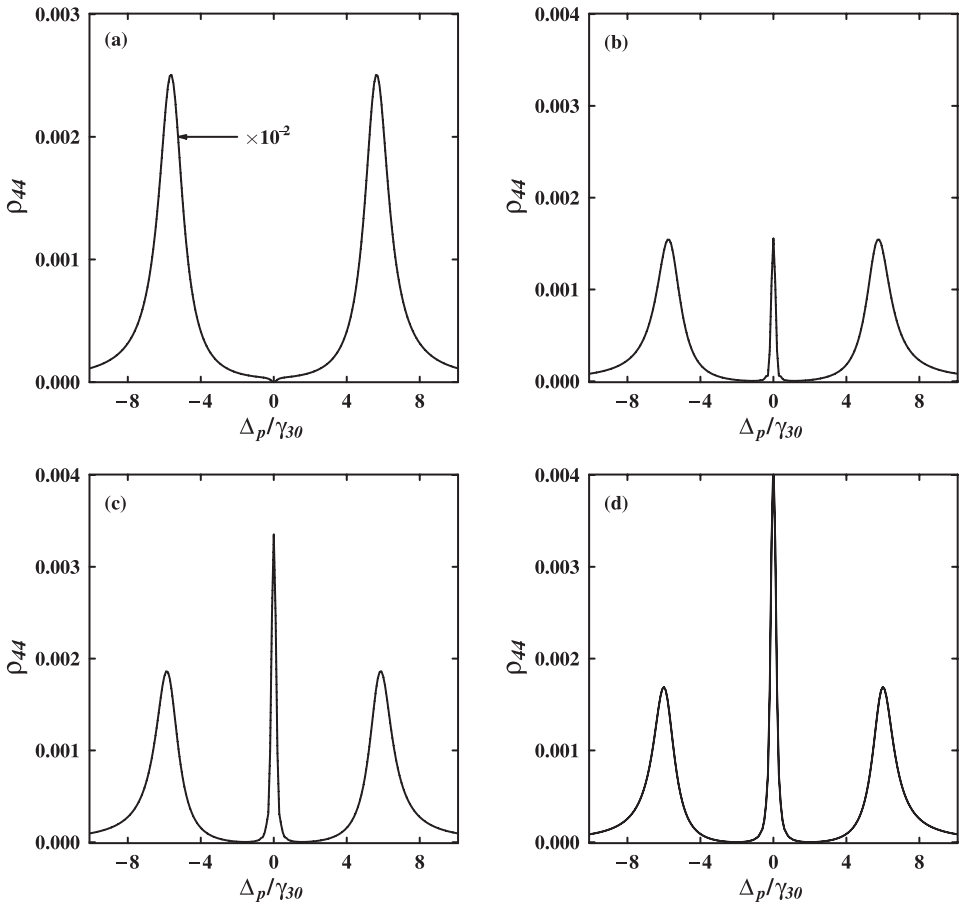

Fig. 2. Two-photon absorption ρ_{44} versus frequency detuning Δ_p. (a) $\Delta_c = \Delta_d = 0$; (b) $\Delta_c = -\gamma_{30}$ and $\Delta_d = \gamma_{30}$; (c) $\Delta_c = -1.5\gamma_{30}$ and $\Delta_d = 1.5\gamma_{30}$; (d) $\Delta_c = -2\gamma_{30}$ and $\Delta_d = 2\gamma_{30}$. Other parameters are chosen as $\Omega_p = 0.1\gamma_{30}$, $\Omega_s = 0.2\gamma_{30}$, $\Omega_c = \Omega_d = 4\gamma_{30}$, $\Delta_s = 0$, $\gamma_{31} = \gamma_{32} = \gamma_{30}$, and $\gamma_{43} = 0.4\gamma_{30}$, respectively.

$$
\begin{aligned}
\dot{\rho}_{02} &= i\left(\Delta_p - \Delta_c\right)\rho_{02} + i\Omega_p\rho_{32} - i\Omega_c\rho_{03},\\
\dot{\rho}_{03} &= -\left(\frac{\gamma_{30}+\gamma_{31}+\gamma_{32}}{2} - i\Delta_p\right)\rho_{03} + i\Omega_p\left(\rho_{33}-\rho_{00}\right)\\
&\quad - i\Omega_s\rho_{04} - i\Omega_c\rho_{02} - i\Omega_d\rho_{01},\\
\dot{\rho}_{04} &= -\left[\frac{\gamma_{43}}{2} - i\left(\Delta_p+\Delta_s\right)\right]\rho_{04} + i\Omega_p\rho_{34} - i\Omega_s\rho_{03},\\
\dot{\rho}_{12} &= i\left(\Delta_d - \Delta_c\right)\rho_{12} + i\Omega_d\rho_{32} - i\Omega_c\rho_{13},\\
\dot{\rho}_{13} &= -\left(\frac{\gamma_{30}+\gamma_{31}+\gamma_{32}}{2} - i\Delta_d\right)\rho_{13} + i\Omega_d\left(\rho_{33}-\rho_{11}\right)\\
&\quad - i\Omega_p\rho_{10} - i\Omega_s\rho_{14} - i\Omega_c\rho_{12},\\
\dot{\rho}_{14} &= -\left[\frac{\gamma_{43}}{2} - i\left(\Delta_d+\Delta_s\right)\right]\rho_{14} + i\Omega_d\rho_{34} - i\Omega_s\rho_{13},\\
\dot{\rho}_{23} &= -\left(\frac{\gamma_{30}+\gamma_{31}+\gamma_{32}}{2} - i\Delta_c\right)\rho_{23} + i\Omega_c\left(\rho_{33}-\rho_{22}\right)\\
&\quad - i\Omega_p\rho_{20} - i\Omega_s\rho_{24} - i\Omega_d\rho_{21},\\
\dot{\rho}_{24} &= -\left[\frac{\gamma_{43}}{2} - i\left(\Delta_c+\Delta_s\right)\right]\rho_{24} + i\Omega_c\rho_{34} - i\Omega_s\rho_{23},\\
\dot{\rho}_{34} &= -\left(\frac{\gamma_{30}+\gamma_{31}+\gamma_{32}+\gamma_{43}}{2} - i\Delta_s\right)\rho_{34}\\
&\quad + i\Omega_s\left(\rho_{44}-\rho_{33}\right) + i\Omega_p\rho_{04} + i\Omega_c\rho_{24} + i\Omega_d\rho_{14}, \quad (2)
\end{aligned}
$$

where the overdots denote the derivative with respect to time t and we have assumed that all involving Rabi frequencies are real without loss of generality. Closure of this atomic system requires that $\sum_{j=0}^{4}\rho_{jj} = 1$ and $\rho_{ij} = \rho_{ji}^{*}$. As it is well-known, the two-photon absorption for the pathway $|0\rangle \rightarrow |3\rangle \rightarrow |4\rangle$ is proportional to the population distribution in the upper excited state $|4\rangle$, i.e., σ_{44}. In the following, we begin with investigating the response of two-photon absorption by solving the density matrix equations (2) numerically in the steady-state limit via a nice Matematica code. Note that, in this paper, all involving parameters are scaled by γ_{30}, which should be in the order of MHz for rubidium or sodium atoms.

First of all, we will analyze how the interference of the dark resonance modifies the two-photon absorption spectra via the numerical calculations based on equation (2) in the steady-state limit. In Figure 2, we plot the two-photon absorption ρ_{44} as a function of probe detuning Δ_p with different frequency detuning of the two coupling fields Δ_c and Δ_d, while keeping other parameters unchanged. It is easy to see from Figure 2 that, the spectra of the two-photon absorption have a convert from single two-photon transparency window at central frequency to double two-photon transparency windows at two different

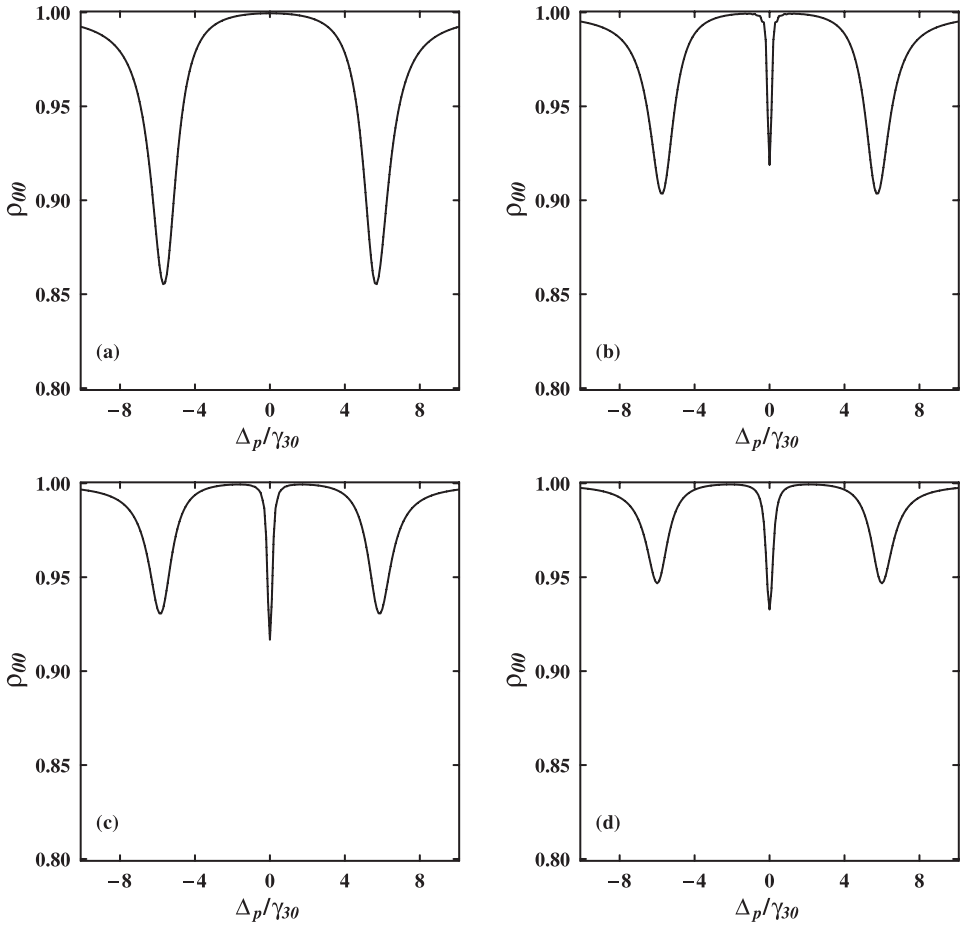

Fig. 3. Population ρ_{00} at the level $|0\rangle$ versus frequency detuning Δ_p. (a) $\Delta_c = \Delta_d = 0$; (b) $\Delta_c = -\gamma_{30}$ and $\Delta_d = \gamma_{30}$; (c) $\Delta_c = -1.5\gamma_{30}$ and $\Delta_d = 1.5\gamma_{30}$; (d) $\Delta_c = -2\gamma_{30}$ and $\Delta_d = 2\gamma_{30}$. Other parameters are chosen as $\Omega_p = 0.1\gamma_{30}$, $\Omega_s = 0.2\gamma_{30}$, $\Omega_c = \Omega_d = 4\gamma_{30}$, $\Delta_s = 0$, $\gamma_{31} = \gamma_{32} = \gamma_{30}$, and $\gamma_{43} = 0.4\gamma_{30}$, respectively.

side frequencies, moreover the position and width of two-frequency EIT windows depends strongly on the frequency detuning of these two coupling fields. Specifically, for the case that the two coupling fields interacts resonantly with the corresponding transitions $|1\rangle \leftrightarrow |3\rangle$ and $|2\rangle \leftrightarrow |3\rangle$, i.e., $\Delta_d = \Delta_c = 0$ [see Fig. 2a], the two-photon absorption can be completely suppressed and the atomic system becomes transparency only at $\Delta_p = 0$. In contrast, when the frequency detuning is varied, for the case that $\Delta_d = -\Delta_c = \gamma_{30}$ [see Fig. 2b], the effect of the frequency detuning is seen to cause a further splitting in each of the dynamic Stark components and gives rise to a three-peak spectral feature with one narrow central line and two symmetrical normal width side lines. There appear double electromagnetically induced two-photon transparency windows. When the coupling-field frequency detuning continues to increase [e.g., $\Delta_d = -\Delta_c = 1.5\gamma_{30}$ and $\Delta_d = -\Delta_c = 2\gamma_{30}$ in Figs. 2c and 2d], the height of the narrow central spectral line can be enhanced remarkably, meantime the height of two side spectral lines with normal width change slowly. As a result, we can see that by adjusting the frequency detuning of the coupling field, such as $\Delta_d = -\Delta_c = 2\gamma_{30}$ [see Fig. 2d], large enhancement of the ultranarrow line can be achieved in the two-photon absorption spectra. Alternatively, the distance between the double two-photon transparency windows becomes larger with increasing Δ_d and Δ_c, that is to say, there is an overall shift of the positions of transparency windows at the opposite direction. These results will be well explained in the later part. In order to further verify that the population ρ_{00} at the level $|0\rangle$ is not equal to zero, the corresponding curves in Figure 3 is clearly presented.

In Figure 4, we plot the two-photon absorption ρ_{44} as a function of probe detuning Δ_p with two different intensities of the coupling fields $\Omega_c = \Omega_d = 2\gamma_{30}$ and $4\gamma_{30}$ in the steady-state limit, while keeping other parameters unchanged. We find that if the coupling-field frequency detuning is fixed (e.g., $\Delta_d = -\Delta_c = \gamma_{30}$), the positions of zero two-photon absorption at two different frequencies are kept unchanged no matter how we vary the intensities of the two coupling fields, but the regimes of two-frequency EIT windows are enlarged and two side spectral lines keep away from each other with increasing Ω_c and Ω_d. This suggests that the positions of zero two-photon absorption at two different frequencies depend sensitively on the frequency detuning of the two coupling coherent fields, but be independent of their intensities. In order to explicitly show the influence of frequency detuning

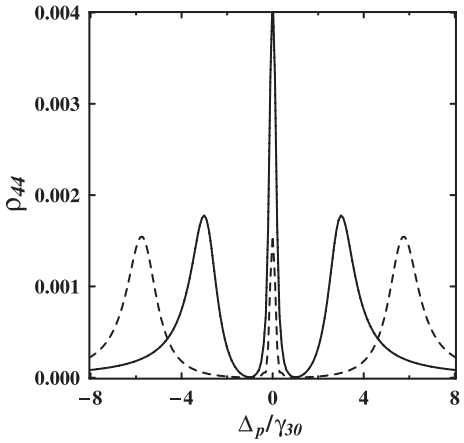

Fig. 4. Two-photon absorption ρ_{44} versus frequency detuning Δ_p for the different intensities of the coupling field: $\Omega_c = \Omega_d = 2\gamma_{30}$ (sold curve) and $\Omega_c = \Omega_d = 4\gamma_{30}$ (dashed curve). Other parameters are chosen as $\Omega_p = 0.1\gamma_{30}$, $\Omega_s = 0.2\gamma_{30}$, $\Delta_s = 0$, $\Delta_d = -\Delta_c = \gamma_{30}$, $\gamma_{31} = \gamma_{32} = \gamma_{30}$, and $\gamma_{43} = 0.4\gamma_{30}$, respectively.

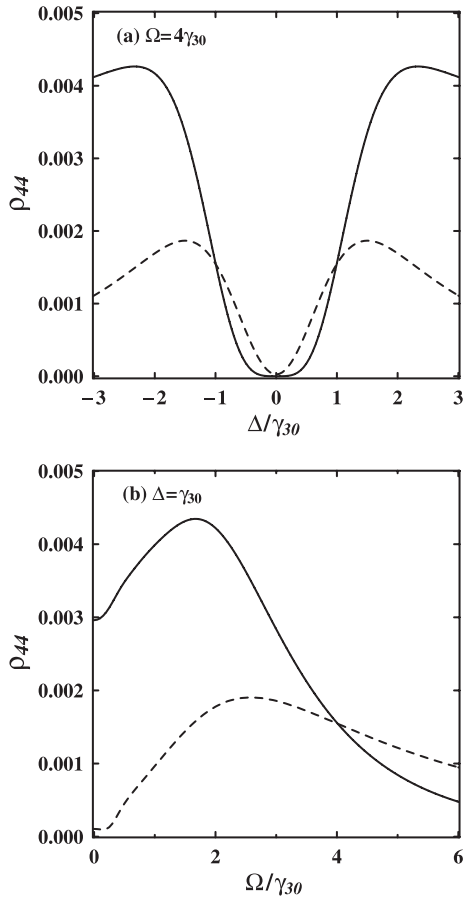

Fig. 5. Two-photon absorption ρ_{44} versus (a) frequency detuning Δ ($\Delta_d = -\Delta_c = \Delta$) and (b) Rabi frequency Ω ($\Omega_c = \Omega_d = \Omega$) for one central peak (sold curve: $\Delta_p = 0$) and two side peaks (dashed curve: $\Delta_p = \pm\sqrt{\Delta^2 + 2\Omega^2}$). Other parameters are chosen as $\Omega_p = 0.1\gamma_{30}$, $\Omega_s = 0.2\gamma_{30}$, $\Delta_s = 0$, $\gamma_{31} = \gamma_{32} = \gamma_{30}$, and $\gamma_{43} = 0.4\gamma_{30}$, respectively.

($\Delta_d = -\Delta_c = \Delta$) and Rabi frequencies ($\Omega_c = \Omega_d = \Omega$) of the two coupling fields on the central and side peaks, in Figures 5a and 5b we plot the two-photon absorption spectra for one central peak (solid cure: $\Delta_p = 0$) and two side peaks (dashed curve: $\Delta_p = \pm\sqrt{\Delta^2 + 2\Omega^2}$), respectively.

In order to further give the explicit explanations of the above results from numerical calculations based on equation (2), we will turn our attention to the dressed-state picture, generated by the two coherent coupling fields Ω_c and Ω_d, namely, the $|1\rangle \leftrightarrow |3\rangle \leftrightarrow |2\rangle$ transitions together with the two coupling fields are treated as a coupled "atom+field" system and the energy levels of the dressed states form a ladder of triplets as shown in Figure 1b. It is obvious that bare-state level $|3\rangle$ should be split into three dressed-state sublevels $|\pm\rangle_3$ and $|0\rangle_3$. Such a subsystem is described by the interaction Hamiltonian $V = \Delta_d|1\rangle\langle 1| + \Delta_c|2\rangle\langle 2| + (\Omega_d|3\rangle\langle 1| + \Omega_c|3\rangle\langle 2| + h.c.)$. The energy eigenvalues of the three dressed states for the case that $\Delta_d = -\Delta_c = \Delta$ and $\Omega_c = \Omega_d = \Omega$ are given by

$$\lambda_\pm = \pm\sqrt{\Delta^2 + 2\Omega^2} \qquad \text{and} \qquad \lambda_0 = 0. \tag{3}$$

The corresponding energy eigenstates are written as

$$|+\rangle_3 = \frac{1}{2\sqrt{\Delta^2 + 2\Omega^2}}\left[2\Omega|3\rangle - \left(\Delta - \sqrt{\Delta^2 + 2\Omega^2}\right)|2\rangle + \left(\Delta + \sqrt{\Delta^2 + 2\Omega^2}\right)|1\rangle\right], \tag{4a}$$

$$|0\rangle_3 = \frac{1}{\sqrt{\Delta^2 + 2\Omega^2}}\left(-\Delta|3\rangle - \Omega|2\rangle + \Omega|1\rangle\right), \tag{4b}$$

$$|-\rangle_3 = \frac{1}{2\sqrt{\Delta^2 + 2\Omega^2}}\left[2\Omega|3\rangle - \left(\Delta + \sqrt{\Delta^2 + 2\Omega^2}\right)|2\rangle + \left(\Delta - \sqrt{\Delta^2 + 2\Omega^2}\right)|1\rangle\right]. \tag{4c}$$

When the frequency detuning of the probe field is tuned at $\Delta_p = \lambda_+$, 0 and λ_-, three stepwise resonant two-photon excitations happen through the channels in the dressed-state basis: $|0\rangle \xrightarrow{\Omega_p} |-\rangle_3 \xrightarrow{\Omega_s} |4\rangle$, $|0\rangle \xrightarrow{\Omega_p} |0\rangle_3 \xrightarrow{\Omega_s} |4\rangle$, and $|0\rangle \xrightarrow{\Omega_p} |+\rangle_3 \xrightarrow{\Omega_s} |4\rangle$, which correspond to the left-side, central, and right-side peaks showed in Figures 2 and 4, respectively. Then the distance between the left and right side peaks is $\delta = \lambda_+ - \lambda_- = 2\sqrt{\Delta^2 + 2\Omega^2}$. This explains that the distance between the two side-peaks increases with the frequency detuning and the Rabi frequency of the two coupling fields. The central peak corresponding to the two-photon absorption in the channel $|0\rangle \xrightarrow{\Omega_p} |0\rangle_3 \xrightarrow{\Omega_s} |4\rangle$ stands at rest at $\Delta_p = 0$ for the altering intensities of the two coupling fields. The double two-photon transparency is induced by the quantum interference among the three coherent two-photon excitation pathways. This can be demonstrated by the probability of the two-photon

absorption according to equations (4a–4c):

$$
\begin{aligned}
P_2 = \frac{2\pi}{\hbar} \Bigg| & \frac{\langle 0|\vec{d}\cdot\vec{E}_p|+\rangle_{3\,3}\langle +|\vec{d}\cdot\vec{E}_s|4\rangle}{E_+ - \hbar\omega_p} \\
& + \frac{\langle 0|\vec{d}\cdot\vec{E}_p|0\rangle_{3\,3}\langle 0|\vec{d}\cdot\vec{E}_s|4\rangle}{E_0 - \hbar\omega_p} \\
& + \frac{\langle 0|\vec{d}\cdot\vec{E}_p|-\rangle_{3\,3}\langle -|\vec{d}\cdot\vec{E}_s|4\rangle}{E_- - \hbar\omega_p} \Bigg|^2 \\
& \times \delta\left(\hbar\omega_4 - \hbar\omega_0 - \hbar\omega_p - \hbar\omega_s\right), \\
= 2\pi & \left| \frac{1}{\Delta^2 + 2\Omega^2} \left(\frac{\Omega^2}{\Delta_p + \lambda_+} + \frac{\Delta^2}{\Delta_p + \lambda_0} + \frac{\Omega^2}{\Delta_p + \lambda_-} \right) \right|^2 \\
& \times \left| \langle 0|\vec{d}\cdot\vec{E}_p|3\rangle\langle 3|\vec{d}\cdot\vec{E}_s|4\rangle \right|^2 \delta\left(\omega_4 - \omega_0 - \omega_p - \omega_s\right),
\end{aligned}
\tag{5}
$$

where $E_i = \hbar\omega_p + \hbar\Delta_p + \hbar\lambda_i$ $(i = +, 0, -)$ represents the relative eigenvalue of the ith dressed state $|i\rangle_3$ to the ground state $|0\rangle$. The occurrence of the minimum in two-photon absorption requires that the part in the first absolute-value bracket on the right-hand side of equation (5) should be equal to vanish, which leads to the following condition after some algebra

$$
\left(\Delta_p^2 - \Delta^2\right)\left(\Delta^2 + 2\Omega^2\right) = 0, \quad \text{i.e.,} \quad \Delta_p = \pm\Delta, \tag{6}
$$

on the basis of the above analysis, we clearly see that when $\Delta_d = -\Delta_c = \Delta$ and $\Omega_c = \Omega_d = \Omega$, the two-photon absorption has minima at $\Delta_p = \pm\Delta$ (EIT windows) and maxima at $\Delta_p = 0$ (central peak) and $\Delta_p = \pm\sqrt{\Delta^2 + 2\Omega^2}$ (two side peaks or Autler-Townes peaks). This can explain why the minimum in two-photon absorption is always located at $\Delta_p = 0$, $\pm\gamma_{30}$, $\pm 1.5\gamma_{30}$, and $\pm 2\gamma_{30}$ in Figures 2 and at $\Delta_p = \pm\gamma_{30}$ in Figure 4.

Now we give a brief discussion about the possible experimental realization of our proposed scheme by means of alkali-metal atoms and appropriate diode lasers. Specifically, we consider for instance the cold atoms ^{87}Rb (nuclear spin $I = 3/2$) on the $5S - 5P - 5D$ transitions as a possible candidate. The designated states can be chosen as follows: $|0\rangle = |5S_{1/2}, F = 1, m_F = 1\rangle$, $|1\rangle = |5S_{1/2}, F = 1, m_F = -1\rangle$, $|2\rangle = |5S_{1/2}, F = 2, m_F = 0\rangle$, $|3\rangle = |5P_{1/2}, F = 2, m_F = 1\rangle$, and $|4\rangle = |5D_{3/2}, F = 3, m_F = 1\rangle$, respectively. In this case, the coherent probe, signal and coupling laser radiations, whose wavelengths are, respectively, 795 nm ($|0\rangle \leftrightarrow |3\rangle$, $|1\rangle \leftrightarrow |3\rangle$, and $|2\rangle \leftrightarrow |3\rangle$) and 762 nm ($|3\rangle \leftrightarrow |4\rangle$), can be obtained from external cavity diode lasers. The probe and signal fields E_p and E_s is linearly polarized light, other two coupling fields E_c and E_d are right and left circularly polarized light, respectively. Moreover, in order to eliminate the Doppler broadening effect, atoms should be trapped and cooled by the magneto-optical trap (MOT) technique.

In summary, we have analyzed and discussed the features of the two-photon absorption spectra in a five-level atomic system in the presence of the interacting double dark resonances. Via numerical simulations we clearly show that the two-photon absorption can be completely suppressed at two different frequencies and the atomic system exhibits double electromagnetically induced transparency windows against the two-photon absorption. The position and width of two-frequency transparency windows can be manipulated via appropriately adjusting the frequency detuning and the intensities of the two coupling fields. Clearly this control of the two-photon absorption should be of importance in the context of related issues like two-photon lasing, pulse-preserving propagation in dissipative media and two-photon entanglement in quantum computing and information processing. More interestingly, one narrow or ultranarrow central spectral line with high amplitude can be achieved in such a system, which has potential application for precision spectroscopy. Form a physical point of view, we well explain these results in terms of quantum interference induced by three different two-photon excitation channels in the dressed-state picture. According to our analysis, these interesting phenomena should be observable in realistic experiments by using alkali-metal atoms (e.g., cold Rb or Na atoms) and appropriate diode lasers.

The research is supported in part by the National Natural Science Foundation of China (Grant Nos. 10575040, 90503010, and 10634060) and by National Basic Research Program of China under Contract No. 2005CB724508. We would like to thank Professor Ying Wu for helpful discussion and his encouragement.

References

1. S.E. Harris, J.E. Field, A. Imamoğlu, Phys. Rev. Lett. **64**, 1107 (1990)
2. Y. Wu, J. Saldana, Y. Zhu, Phys. Rev. A **67**, 013811 (2003); Y. Wu, L. Wen, Y. Zhu, Opt. Lett. **28**, 631 (2003)
3. L. Deng, M. Kozuma, E.W. Hagley, M.G. Payne, Phys. Rev. Lett. **88**, 143902 (2002); L. Deng, M.G. Payne, Phys. Rev. Lett. **91**, 243902 (2003)
4. A.S. Zibrov, M.D. Lukin, L. Hollberg, M.O. Scully, Phys. Rev. A **65**, 051801(R) (2002); A.S. Zibrov, A.B. Matsko, M.O. Scully, Phys. Rev. Lett. **89**, 103601 (2002)
5. S.E. Harris, L.V. Hau, Phys. Rev. Lett. **82**, 4611 (1999)
6. Y. Niu, R. Li, S. Gong, Phys. Rev. A **71**, 043819 (2005)
7. W. Yang, S. Gong, Y. Niu, S. Jin, Z. Xu, J. Phys. B **38**, 2657 (2005)
8. M.D. Lukin, S.F. Yelin, M. Fleischhauer, Phys. Rev. Lett. **84**, 4232 (2000); M. Fleischhauer, M.D. Lukin, Phys. Rev. Lett. **84**, 5094 (2000); M. Fleischhauer, M.D. Lukin, Phys. Rev. A **65**, 022314 (2002); for a review, see M.D. Lukin, Rev. Mod. Phys. **75**, 457 (2003); M. Fleischhauer, A. Imamoglu, J.P. Marangos, Rev. Mod. Phys. **77**, 633 (2005)
9. G.S. Agarwal, W. Harshawardhan, Phys. Rev. Lett. **77**, 1039 (1996)
10. J.Y. Gao, S.H. Yang, D. Wang, X.Z. Guo, K.X. Chen, Y. Jiang, B. Zhao, Phys. Rev. A **61**, 023401 (2000)
11. D. McGloin, J. Phys. B **36**, 2861 (2003)
12. M.A. Antón, O.G. Calderón, F. Carreño, Phys. Rev. A **72**, 023809 (2005)

13. J.H. Wu, A.J. Li, Y. Ding, Y.C. Zhao, J.Y. Gao, Phys. Rev. A **72**, 023802 (2005)
14. S.Y. Zhu, M.O. Scully, Phys. Rev. Lett. **76**, 388 (1996); S.Y. Zhu, R.C.F. Chan, C.P. Lee, Phys. Rev. A **52**, 710 (1995); S.Y. Zhu, L.M. Narducci, M.O. Scully, Phys. Rev. A **52**, 4791 (1995)
15. S. Menon, G.S. Agarwal, Phys. Rev. A **61**, 013807 (2000)
16. S. Menon, G.S. Agarwal, Phys. Rev. A **57**, 4014 (1998); S. Menon, G.S. Agarwal, Phys. Rev. A **59**, 740 (1999); G.S. Agarwal, Phys. Rev. A **55**, 2467 (1997)
17. P. Zhou, S. Swain, Phys. Rev. Lett. **77**, 3995 (1996); P. Zhou, S. Swain, Phys. Rev. Lett. **78**, 832 (1997)
18. T. Hong, Phys. Rev. Lett. **90**, 183901 (2003); Y. Wu, L. Deng, Phys. Rev. Lett. **93**, 143904 (2004); L. Deng, M.G. Payne, G. Huang, E.W. Hagley, Phys. Rev. E **72**, 055601(R) (2005); G. Huang, L. Deng, M.G. Payne, Phys. Rev. E **72**, 016617 (2005)
19. E. Paspalakis, N.J. Kylstra, P.L. Knight, Phys. Rev. Lett. **82**, 2079 (1999); E. Paspalakis, N.J. Kylstra, P.L. Knight, Phys. Rev. A **61**, 045802 (2000)
20. E. Paspalakis, P.L. Knight, Phys. Rev. Lett. **81**, 293 (1998); E. Paspalakis, Z. Kis, Phys. Rev. A **66**, 025802 (2002); A. Fountoulakis, A.F. Terzis, E. Paspalakis, Phys. Rev. A **73**, 033811 (2006)
21. H. Kang, Y. Zhu, Phys. Rev. Lett. **91**, 093601 (2003)
22. M. Yan, E.G. Rickey, Y. Zhu, Phys. Rev. A **64**, 043807 (2001)
23. M. Yan, E. Rickey, Y. Zhu, Opt. Lett. **26**, 548 (2001)
24. Y. Wu, M.G. Payne, E.W. Hagley, L. Deng, Opt. Lett. **29**, 2294 (2004)
25. J.H. Zou, X.M. Hu, G.L. Cheng, X. Li, D. Du, Phys. Rev. A **72**, 055802 (2005)
26. M.D. Lukin, S.F. Yelin, M. Fleischhauer, M.O. Scully, Phys. Rev. A **60**, 3225 (1999)
27. Y.C. Chen, Y.A. Liao, H.Y. Chiu, J.J. Su, I.A. Yu, Phys. Rev. A **64**, 053806 (2001)
28. Y. Niu, S. Gong, R. Li, S. Jin, Phys. Rev. A **70**, 023805 (2004)
29. C.Y. Ye, A.S. Zibrov, Y.V. Rostovtsev, M.O. Scully, Phys. Rev. A **65**, 043805 (2002)
30. S.F. Yelin, V.A. Sautenkov, M.M. Kash, G.R. Welch, M.D. Lukin, Phys. Rev. A **68**, 063801 (2003)
31. C. Goren, A.D. Wilson-Gordon, M. Rosenbluh, H. Friedmann, Phys. Rev. A **69**, 063802 (2004)
32. E. Paspalakis, N.J. Kylstra, P.L. Knight, Phys. Rev. A **65**, 053808 (2002); E. Paspalakis, P.L. Knight, J. Opt. B: Quantum Semiclass. Opt. **4**, 372 (2002)
33. M.O. Scully, M.S. Zubairy, *Quantum Optics* (Cambridge University Press, Cambridge, 1997), Chap. 5